

THE TOP QUARK

Updated December 2011 by T.M. Liss (Univ. Illinois) and A. Quadt (Univ. Göttingen).

A. Introduction: The top quark is the $Q = 2/3$, $T_3 = +1/2$ member of the weak-isospin doublet containing the bottom quark (see the review on the “Electroweak Model and Constraints on New Physics” for more information). This note summarizes the properties of the top quark (mass, production cross section, decay branching ratios, *etc.*), and provides a discussion of the experimental and theoretical issues involved in their determination

B. Top quark production at the Tevatron and LHC:

In hadron collisions, top quarks are produced dominantly in pairs through the QCD processes $q\bar{q} \rightarrow t\bar{t}$ and $gg \rightarrow t\bar{t}$. In $p\bar{p}$ collisions at the Tevatron with $\sqrt{s} = 1.96$ TeV the most recent calculations are at NLO with next-to-leading-log soft gluon resummation [1], and at approximate next-to-next-to-leading order (NNLO) [2]. Cacciari *et al.* give a production cross section of 7.93 pb for $m_t = 172.5$ GeV/ c^2 with MRST2006nnlo PDFs. Over the range 150 GeV/ $c^2 \leq m_t \leq 190$ GeV/ c^2 the calculated cross section changes by approximately 0.24 pb/(GeV/ c^2) for m_t greater or less than 172.5 GeV/ c^2 . An approximate NNLO calculation by Kidonakis and Vogt yields a production cross section of 7.68 pb for $m_t = 172.5$ GeV/ c^2 using MRST2006nnlo, with nearly the same mass-dependence. The difference in the central value obtained using different PDFs is typically a few tenths of a pb or less. Langenfeld *et al.* [3], in an approximate NNLO calculation find 7.04 pb for $m_t = 173$ GeV/ c^2 using MSTW2008nnlo. The uncertainties on these calculations, due to the choice of scale, which is set at $\mu = m_t$, are typically 0.5 pb or less. In pp collisions at the LHC with $\sqrt{s} = 7$ TeV, Langenfeld *et al.* calculate an approximate NNLO production cross section of 161 pb for $m_t = 172.5$ GeV/ c^2 using CTEQ6.6 with an uncertainty of less than 10%. Approximately 85% of the production cross section at the Tevatron is from $q\bar{q}$ annihilation, with the remainder from gluon-gluon fusion [4], while at LHC energies about 90% of the production is from the

latter process at $\sqrt{s} = 14$ TeV ($\approx 80\%$ at $\sqrt{s} = 7$ TeV). The resulting theoretical prediction of the top quark cross-section at the LHC is $\sigma_{t\bar{t}} = 165_{-16}^{+11}$ pb, assuming a top quark mass of 172.5 GeV/ c^2 [5].

Somewhat smaller cross sections are expected from electroweak single top production mechanisms, namely from $q\bar{q}' \rightarrow t\bar{b}$ [6] and $qb \rightarrow q't$ [7], mediated by virtual s -channel and t -channel W bosons, respectively. At the Tevatron, the production cross sections of top and antitop are identical, while at the LHC they are not. Approximate NNLO cross sections for t -channel single top quark production are calculated for $m_t = 173$ GeV/ c^2 to be 1.04 pb in $p\bar{p}$ collisions at $\sqrt{s} = 1.96$ TeV and 41.7 pb in pp collisions at $\sqrt{s} = 7$ TeV [8]. For the s -channel, these calculations yield 0.52 pb for the Tevatron, and 3.2 pb for $\sqrt{s} = 7$ TeV LHC [9]. The corresponding single *anti*-top-quark cross sections at the LHC are 22.5 pb and 1.4 pb for t - and s -channel, respectively, at $\sqrt{s} = 7$ TeV. At LHC energies, the production of a single top quark in association with a W^- boson, through $bg \rightarrow W^-t$, becomes relevant. At $\sqrt{s} = 7$ TeV, an approximate NNLO calculation using the MSTW2008 PDF gives 8.1 pb [10]. The production cross section for single *anti*-top quarks in this channel ($W^+\bar{t}$) is the same as for single top quarks.

The cross sections for single top production are proportional to $|V_{tb}|^2$, and no assumption is needed on the number of quark families or on the unitarity of the CKM matrix in extracting $|V_{tb}|$. Separate measurements of the s - and t -channel processes provide sensitivity to physics beyond the Standard Model (SM) [11].

The identification of top quarks in the electroweak single-top channel is much more difficult than in the QCD $t\bar{t}$ channel, due to a less distinctive signature and significantly larger backgrounds.

In top decay, the Ws and Wd final states are expected to be suppressed relative to Wb by the square of the CKM matrix elements V_{ts} and V_{td} . Assuming unitarity of the three-generation CKM matrix, these matrix element values are estimated to be less than 0.043 and 0.014, respectively, implying a value of

$V_{tb} > 0.999$ (see the review “The CKM Quark-Mixing Matrix” for more information). With a mass above the Wb threshold, and V_{tb} close to unity, the decay width of the top quark is expected to be dominated by the two-body channel $t \rightarrow Wb$. Neglecting terms of order m_b^2/m_t^2 , α_s^2 , and $(\alpha_s/\pi)M_W^2/m_t^2$, the width predicted in the Standard Model (SM) at NLO is [12]:

$$\Gamma_t = \frac{G_F m_t^3}{8\pi\sqrt{2}} \left(1 - \frac{M_W^2}{m_t^2}\right)^2 \left(1 + 2\frac{M_W^2}{m_t^2}\right) \left[1 - \frac{2\alpha_s}{3\pi} \left(\frac{2\pi^2}{3} - \frac{5}{2}\right)\right], \quad (1)$$

where m_t refers to the top quark pole mass. The width for a value of $m_t = 171 \text{ GeV}/c^2$, close to the world average, is $1.29 \text{ GeV}/c^2$ (we use $\alpha_s(M_Z) = 0.118$) and increases with mass. With its correspondingly short lifetime of $\approx 0.5 \times 10^{-24} \text{ s}$, the top quark is expected to decay before top-flavored hadrons or $t\bar{t}$ -quarkonium-bound states can form [13]. The order α_s^2 QCD corrections to Γ_t are also available [14], thereby improving the overall theoretical accuracy to better than 1%.

The final states for the leading pair-production process can be divided into three classes:

- A. $t\bar{t} \rightarrow W^+ b W^- \bar{b} \rightarrow q \bar{q}' b q'' \bar{q}''' \bar{b}$, (45.7%)
- B. $t\bar{t} \rightarrow W^+ b W^- \bar{b} \rightarrow q \bar{q}' b \ell^- \bar{\nu}_\ell \bar{b} + \ell^+ \nu_\ell b q'' \bar{q}''' \bar{b}$, (43.8%)
- C. $t\bar{t} \rightarrow W^+ b W^- \bar{b} \rightarrow \bar{\ell} \nu_\ell b \ell' \bar{\nu}_{\ell'} \bar{b}$. (10.5%)

The quarks in the final state evolve into jets of hadrons. A, B, and C are referred to as the all-jets, lepton+jets (ℓ +jets), and dilepton ($\ell\ell$) channels, respectively. Their relative contributions, including hadronic corrections, are given in parentheses assuming lepton universality. While ℓ in the above processes refers to e , μ , or τ , most of the results to date rely on the e and μ channels. Therefore, in what follows, we will use ℓ to refer to e or μ , unless otherwise noted.

The initial and final-state quarks can radiate gluons that can be detected as additional jets. The number of jets reconstructed in the detectors depends on the decay kinematics, as well as on the algorithm for reconstructing jets used by the analysis. The transverse momenta of neutrinos are reconstructed from the imbalance in transverse momentum measured in each event (missing p_T , which is here also missing E_T).

NLO Monte Carlo programs are available for the $t\bar{t}$ production processes [15]. Theoretical estimates of the background processes (W or Z bosons+jets and dibosons+jets) using leading order (LO) calculations have large uncertainties. While this limitation affects estimates of the overall production rates, it is believed that the LO determination of event kinematics, and of the fraction of W +multi-jet events that contain b - or c -quarks, are relatively accurate [16]. Comparison to CDF and DØ data, however, indicates the b - and c -quark fractions to be underestimated by the LO generators and hence does not seem to support the theoretical expectations.

C. Top quark measurements: Since the discovery of the top quark, direct measurements of $t\bar{t}$ production have been made at three center-of-mass energies, providing stringent tests of QCD. The first measurements were made in Run I at the Tevatron at $\sqrt{s} = 1.8$ TeV. In Run II at the Tevatron relatively precise measurements were made at $\sqrt{s} = 1.96$ TeV. Finally, beginning in 2010 measurements have been made at the LHC at $\sqrt{s} = 7$ TeV.

Production of single top quarks through electroweak production mechanisms has now been measured with good precision at the Tevatron at $\sqrt{s} = 1.96$ TeV, and at the LHC at $\sqrt{s} = 7$ TeV. Recent measurements are beginning to separate the s - and t -channel production cross sections, and at the LHC, the Wt mechanism as well, though only t -channel is well measured to date. The measurements allow an extraction of the CKM matrix element V_{tb} .

The top quark mass is now measured at the 0.6% level, by far the most precisely measured quark mass. Together with the W boson mass measurement, this places strong constraints on the mass of the Standard Model Higgs boson.

With more than 5 fb^{-1} of Tevatron data analyzed as of this writing, and $1 - 2 \text{ fb}^{-1}$ of LHC data, many properties of the top quark are now being measured with precision. These include properties related to the production mechanism, such as $t\bar{t}$ spin correlations, forward-backward or charge asymmetries, and differential production cross sections, as well as properties related to the $t - W - b$ decay vertex, such as the helicity of the

W bosons from the top decay. In addition, many searches for physics beyond the Standard Model are being performed with increasing reach in both production and decay channels.

In the following sections we review the current status of measurements of the characteristics of the top quark.

C.1 Top quark production

C.1.1 $t\bar{t}$ production Fig. 1 summarizes the $t\bar{t}$ production cross-section measurements from both the Tevatron and LHC. The most recent measurement from D0 [17], combining the measurements from the dilepton and lepton plus jets final states in 5.4 fb^{-1} , is $7.56_{-0.56}^{+0.63} \text{ pb}$. From CDF the most precise measurement made recently [18] is in 4.6 fb^{-1} and is a combination of dilepton, lepton plus jets, and all-hadronic final-state measurements, yielding $7.50 \pm 0.48 \text{ pb}$. Both of these measurements assume a top mass of $172.5 \text{ GeV}/c^2$. The dependence of the cross section measurements on the value chosen for the mass is less than that of the theory calculations because it only affects the determination of the acceptance. In some analyses also the shape of topological variables might be modified. At LHC energies, ATLAS [19] combines measurements in the lepton plus jets and dilepton final states with 0.7 fb^{-1} to find $176 \pm 14 \text{ pb}$, whereas a more recent analysis of that dataset in the lepton plus jets channel without b -tagging yields the most precise result of $179 \pm 12 \text{ pb}$ [20] and a measurement in the all-jets channels using 1.02 fb^{-1} yields $167 \pm 80 \text{ pb}$ [21]. CMS [22] uses $0.8 - 1.1 \text{ fb}^{-1}$ in the lepton plus jets channel and measures $164 \pm 14 \text{ pb}$. In the all-hadronic channel they use 1.1 fb^{-1} for a cut-based event selection combined with a kinematic fit and obtain $136 \pm 45 \text{ pb}$ [23]. These should be compared to the theoretical calculations that yield $7.9 - 6.7 \text{ pb}$ for top masses from 170 to $175 \text{ GeV}/c^2$ respectively [1] at $\sqrt{s} = 1.96 \text{ TeV}$ and $\sigma_{t\bar{t}} = 165_{-16}^{+11} \text{ pb}$, assuming $m_t = 172.5 \text{ GeV}/c^2$ at $\sqrt{s} = 7 \text{ TeV}$ at the LHC [5] (see Listings).

Most of these measurements assume a $t \rightarrow Wb$ branching ratio of 100%. CDF and DØ have made direct measurements of the $t \rightarrow Wb$ branching ratio [24]. Comparing the number of events with 0, 1 and 2 tagged b jets in the lepton+jets channel,

and also in the dilepton channel, using the known b -tagging efficiency, the ratio $R = B(t \rightarrow Wb) / \sum_{q=d,s,b} B(t \rightarrow Wq)$ can be extracted. In 5.4 fb^{-1} of data, DØ measures $R = 0.90 \pm 0.04$, 2.5σ from unity. A significant deviation of R from unity would imply either non-SM top decay (for example a flavor-changing neutral-current decay), or a fourth generation of quarks.

CDF also performs measurements of the $t\bar{t}$ production cross section normalized to the Z production cross section in order to reduce the impact of the luminosity uncertainty.

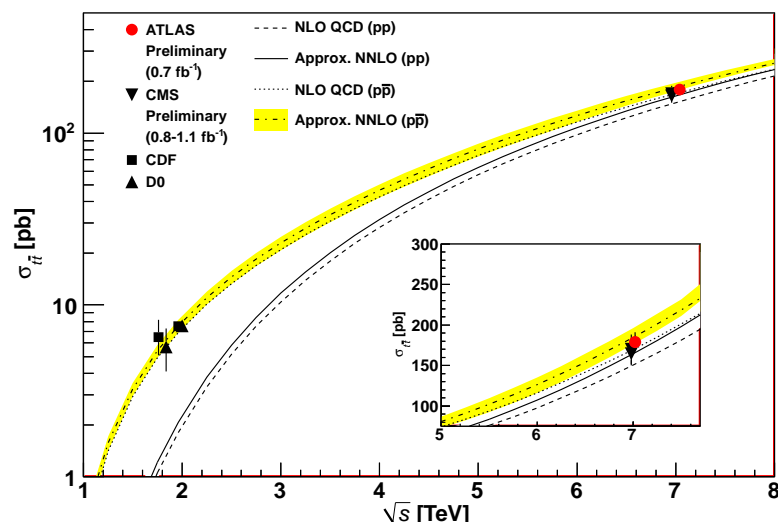


Figure 1: Measured and predicted $t\bar{t}$ production cross sections from Tevatron energies in $p\bar{p}$ collisions to LHC energies in pp collisions. Tevatron data points at $\sqrt{s} = 1.8 \text{ TeV}$ are from Refs. [25] and [26]. Those at $\sqrt{s} = 1.96 \text{ TeV}$ are from Refs. [17] and [18]. The ATLAS and CMS data points are from Refs. [20] and [22], respectively. Theory curves are generated using HATHOR [5] with input from Ref. [27] for the NLO curves and Ref. [2] for the approximate NNLO curves. Figure adapted from Ref. [19].

In Fig. 1, one sees the importance of $p\bar{p}$ at Tevatron energies where the valence antiquarks in the antiprotons contribute to the dominant $q\bar{q}$ production mechanism. At LHC energies the dominant production mode is gluon-gluon fusion and the pp - $p\bar{p}$ difference nearly disappears. The excellent agreement of these measurements with the theory calculations is a strong validation

of QCD and the soft-gluon resummation techniques employed in the calculations. The measurements are not yet precise enough to distinguish between the NLO and approximate NNLO calculations including their respective PDF uncertainties.

C.1.2 Single-top production Single-top quark production was first observed in 2009 by DØ [28] and CDF [29,30] at the Tevatron. The production cross section at the Tevatron is roughly half that of the $t\bar{t}$ cross section, but the final state with a single W -boson and typically two jets is less distinct than that for $t\bar{t}$ and much more difficult to distinguish from the background of W +jets and other sources. A recent review of the first observation and the techniques used to extract the signal from the backgrounds can be found in [31].

The dominant production at the Tevatron is through s -channel and t -channel W -boson exchange. Associated production with a W -boson (Wt production) has a cross section that is too small to observe at the Tevatron. The t -channel process includes $qb \rightarrow q't$ and $qg \rightarrow q't\bar{b}$, while the s -channel process is $q\bar{q}' \rightarrow t\bar{b}$. The s - and t -channel productions can be separated kinematically. This is of particular interest because potential physics beyond the Standard Model, such as fourth-generation quarks, heavy W and Z bosons, or flavor-changing-neutral-currents [11], would affect the s - and t -channels differently. However, the separation is difficult and initial observations and measurements at the Tevatron by both experiments were of combined $s + t$ -channel production. The two experiments combined their measurements for maximum precision with a resulting $s+t$ channel production cross section of $2.76_{-0.47}^{+0.58}$ pb [32]. The measured value assumes a top quark mass of $170 \text{ GeV}/c^2$. The mass dependence of the result comes both from the acceptance dependence and from the $t\bar{t}$ background evaluation. Also the shape of discriminating topological variables is sensitive to m_t . It is therefore not necessarily a simple linear dependence but amounts to only a few tenths of picobarns over the range $170 - 175 \text{ GeV}/c^2$. The measured value agrees well with the theoretical calculation at $m_t = 173 \text{ GeV}/c^2$ of $\sigma_{s+t} = 3.12$ pb (including both top and anti-top production) [8,9].

Both experiments have done separate measurements of the s - and t -channel cross sections by reoptimizing the analysis for one or both of the channels separately. In a simultaneous measurement of s - and t -channel cross sections, CDF measures $\sigma_s = 1.8_{-0.5}^{+0.7}$ pb and $\sigma_t = 0.8_{-0.4}^{+0.4}$ pb, respectively, in 3.2 fb^{-1} of data [30], while DØ measures $2.7_{-0.6}^{+0.7}$ pb and $0.7_{-0.4}^{+0.4}$ pb, respectively in 5.4 fb^{-1} of integrated luminosity [33]. In a separate analysis, optimized for the s -channel alone, CDF measures $1.49_{-0.75}^{+0.92}$ pb in 3.2 fb^{-1} of data [34].

Recently, DØ has measured the t -channel production cross section separately in 5.4 fb^{-1} of data [35] using a variety of advanced analysis techniques similar to those described in [31]. These take advantage of kinematic differences in such things as the leading b -tagged jet p_T , centrality of jets, lepton charge times η of the jets, and the scalar sum of the energy of the final state objects. The s -channel production is considered a background and integrated over the full measured s -channel plane. The $p\bar{p} \rightarrow tqb + X$ cross section is measured to be 2.90 ± 0.59 pb, assuming a top quark mass of $172.5 \text{ GeV}/c^2$. This is in good agreement with the theoretical value at this mass of 2.08 ± 0.13 pb [8]. It should be noted that the theory citations here list cross sections for t or \bar{t} alone, whereas the experiments measure the sum. At the Tevatron these cross sections are equal. The theory values quoted here already include this factor of two.

At the LHC the t -channel cross section is expected to be more than three times as large as s -channel and Wt production, combined. Both ATLAS and CMS have measured single top production cross sections at $\sqrt{s} = 7 \text{ TeV}$ in pp collisions. In the measurement of the t -channel cross section, both experiments treat s -channel and Wt production as backgrounds. ATLAS uses a counting experiment in 0.7 fb^{-1} and combines $W + 2$ and 3 jet data to measure $\sigma_t = 90_{-22}^{+32}$ pb [36]. In 36 pb^{-1} of data, CMS uses a boosted decision tree and kinematic observables to separate signal from background, and combines the two measurements to find $\sigma_t = 83.6 \pm 30.0$ pb [37]. The experimental uncertainties are still too large for a precision test, but the measurements are consistent with the theoretical

expectation of $64.2_{-1.1}^{+1.8}$ pb at $m_t = 173$ GeV/c² [8]. This theoretical value is the sum of the t and \bar{t} production cross sections, which individually are 41.7 pb and 22.5 pb, respectively, at $\sqrt{s} = 7$ TeV.

The s -channel production cross section is expected to be only 4.6 ± 0.3 pb for $m_t = 173$ GeV/c² at $\sqrt{s} = 7$ TeV [9], and has not yet been observed at LHC. The Wt process has also not yet been observed, but appears a bit closer and has a theoretical cross section of 15.6 ± 1.2 pb [10]. This is of interest because it probes the $W - t - b$ vertex in a different kinematic region than s - and t -channel production, and because of its similarity to the associated production of a charged-Higgs boson and a top quark. The signal is difficult to extract because of its similarity to the $t\bar{t}$ signature. Similarly, it is difficult to uniquely define because at NLO a subset of diagrams have the same final state as $t\bar{t}$ and the two interfere [38]. The cross section is calculated using the *diagram removal* technique [39] to define the signal process. In the diagram removal technique the interfering diagrams are removed, at the amplitude level, from the signal definition (an alternate technique, *diagram subtraction* removes these diagrams at the cross-section level and yields similar results). These techniques work provided the selection cuts are defined such that the interference effects are small, which is usually the case.

At ATLAS, a search is performed in 0.7 fb⁻¹ using dilepton decays of the two putative W bosons in the final state and selecting events with exactly one high- p_T jet and large missing E_T [40]. No significant signal is observed yet, and the background-only hypothesis is rejected at only the 1.2σ level. Interpreted as a signal, the measured cross section is 14 ± 11 pb. At CMS a recent result has been released using 2.7 fb⁻¹ of data. CMS also uses the dilepton channel and selects events with at least one high- p_T jet and large missing E_T [41]. The CMS analysis requires exactly one b -tagged jet, which helps to distinguish the signal from non-top backgrounds and from $t\bar{t}$ production. The observed data are inconsistent with the background-only hypothesis at the 2.7σ level. If interpreted as

a signal, the measured cross section is 22_{-7}^{+9} pb, consistent with the theoretical expectation.

The CKM matrix element V_{tb} is extracted from the measured cross sections using the ratio to the theoretical values, which assume $V_{tb} = 1.0$. The extracted value therefore depends on the theoretical cross section. The results, including limits at the 95% C.L., are summarized in Table 1.

Table 1: Measurements and 95% C.L. limits of $|V_{tb}|$ from single-top results.

$ V_{tb} $	Source	$\int \mathcal{L} dt$ (fb^{-1})	Ref.
$ V_{tb} = 0.88 \pm 0.07$	DØ+CDF Run II	2.3-3.2	[32]
$ V_{tb} > 0.77$	DØ+CDF Run II	2.3-3.2	[32]
$ V_{tb} = 1.02_{-0.11}^{+0.10}$	DØ	5.4	[33]
$ V_{tb} = 1.14 \pm 0.22$	CMS	0.036	[37]
$ V_{tb} > 0.62$	CMS	0.036	[37]

C.1.3 Top Quark Forward-Backward & Charge Asymmetry:

NLO calculations predict a small forward-backward asymmetry in $t\bar{t}$ production at the Tevatron of $(\approx 5.0 \pm 1.5)\%$ [42]. The asymmetry arises from an interference between the Born and box diagrams for $t\bar{t}$ production and between diagrams with initial- and final-state gluon radiation. Both CDF and DØ have measured asymmetry values in excess of the SM prediction, fueling speculation about exotic production mechanisms (see, for example, [43] and references therein). The first measurement of this asymmetry by DØ in 0.9 fb^{-1} [44] found an asymmetry at the detector level of $(12 \pm 8)\%$. The first CDF measurement in 1.9 fb^{-1} [45] yielded $(24 \pm 14)\%$ at parton level. Both values were higher, though statistically consistent with the small SM expectation. With the addition of more data, the uncertainties have been reduced, but the measured asymmetries remain in excess of the SM expectation. The most recent measurement from DØ in 5.4 fb^{-1} finds an asymmetry, corrected for detector acceptance and resolution, of $(19.6 \pm 6.5)\%$ [46]. From

CDF, the most recent measurement combines results in the lepton+jets and dilepton channels, using up to 5.3 fb^{-1} , and finds $(20.1 \pm 6.7)\%$ [47]. CDF has recently reported a mass-dependent asymmetry [48], with a larger asymmetry at large $t\bar{t}$ invariant mass. DØ does not see any significant increase at large mass [46].

At LHC, where the dominant $t\bar{t}$ production mechanism is the charge-symmetric gluon-gluon fusion, the measurement is more difficult. For the sub-dominant $q\bar{q}$ production mechanism, the symmetric pp collision does not define a forward and backward direction. Instead, the charge asymmetry is defined in terms of a positive versus a negative $t - \bar{t}$ rapidity difference. Both CMS [49] and ATLAS [50] have made preliminary measurements of the charge asymmetry in almost 1 fb^{-1} . The uncertainties are still too large for a precision test, but both measurements are consistent with the very small asymmetry expected at the LHC while also not being inconsistent with the larger asymmetry observed at the Tevatron.

C.2 Top Quark Properties

C.2.1 Top Quark Mass Measurements: The most precisely studied property of the top quark is its mass. The top mass has been measured in the lepton+jets, the dilepton, and the all-jets channel by both CDF and DØ. At the LHC, both CMS and ATLAS have made measurements in the lepton+jets channel, CMS also in the dilepton channel. The latest results are summarized in Table 2. The lepton+jets channel yields the most precise single measurements because of good signal to background (in particular after b-tagging) and the presence of only a single neutrino in the final state. The momentum of a single neutrino can be reconstructed (up to a quadratic ambiguity) via the missing E_T measurement and the constraint that the lepton and neutrino momenta reconstruct to the known W boson mass.

A large number of techniques have now been applied to measuring the top mass. The original ‘template method’ [51], in which Monte Carlo templates of reconstructed mass distributions are fit to data, has evolved into a precision tool in the lepton+jets channel, where the systematic uncertainty due to

the jet energy scale uncertainty is controlled by a simultaneous, *in situ*, fit to the $W \rightarrow jj$ hypothesis [52]. The latest measurements with this technique, which is now also used in the all-jets channel, are from ATLAS and CDF. In 0.7 fb^{-1} of data in the lepton+jets channel, ATLAS already achieves a total uncertainty of better than 2%, with a statistical component of close to 0.5% [53]. The measurement from CDF with 5.6 fb^{-1} [54] achieves a precision of better than 1% in the lepton+jets channel and is combined with a measurement in the dilepton channel yielding a precision of about 0.8%.

The template method is complemented by the ‘matrix element’ method. This method was first applied by the DØ Collaboration [55], and is similar to a technique originally suggested by Kondo *et al.* [56] and Dalitz and Goldstein [57]. In the matrix element method a probability for each event is calculated as a function of the top mass, using a LO matrix element for the production and decay of $t\bar{t}$ pairs. The *in situ* calibration of dijet pairs to the $W \rightarrow jj$ hypothesis is now also used with the matrix element technique to constrain the jet energy scale uncertainty. The latest measurement with this technique is from DØ in the lepton+jets channel with 3.6 fb^{-1} yielding an uncertainty of about 0.9% [58].

CMS has measured the top mass at LHC using an ‘ideogram’ method, first used by DØ [59], in which a constrained fit is performed and an event-by-event likelihood for signal or background is calculated taking into account all jet-parton assignments. In the lepton+jets channel at CMS, the measurement has a precision of 2% in just 0.036 fb^{-1} . The precision is slightly improved by a combination with a measurement in the dilepton channel.

In the dilepton channel, the signal to background is typically very good, but reconstruction of the mass is non-trivial because there are two neutrinos in the final state, yielding a kinematically unconstrained system. A variety of techniques have been developed to handle this. Recently, an analytic solution to the problem has been proposed [60], but this has not yet been used in the mass measurement. The most precise measurements in the dilepton channel come from the application of the matrix

element technique, in which an integration is performed over the unmeasured neutrino energies. A detailed description of the use of the matrix element technique in the dilepton channel is given in [61]. The most recent measurement in the dilepton channel by DØ uses 5.4 fb^{-1} of data and has a precision of better than 2% [62].

Several other techniques also yield precise measurements in the dilepton channel. In the neutrino weighting technique a weight is assigned by assuming a top mass value and applying energy-momentum conservation to the top decay, resulting in up to four possible pairs of solutions for the neutrino and anti-neutrino momenta. The missing E_T calculated in this way is then compared to the observed missing E_T to assign a weight [63]. Another recent measurement in the dilepton channel uses the Dalitz and Goldstein technique [64]. The precision of these techniques approaches that of the matrix element technique, but the measurements to date have used only 2 fb^{-1} of data.

In the all-jets channel there is no ambiguity due to neutrino momenta, but the signal to background is significantly poorer due to the severe QCD multijets background. The emphasis therefore has been on background modeling, and reduction through event selection. The most recent measurement in the all-jets channel, by CDF in 5.8 fb^{-1} [65], uses a template method for reconstruction and achieves a precision of almost 1%.

A recent measurement from CDF in 5.7 fb^{-1} uses a neural net to select events with a missing E_T plus jets signature [66]. A modified template method is used to extract the top mass, and a precision of about 1.5% is achieved.

The dominant systematic uncertainty in these methods is the understanding of the jet energy scale, and so several techniques have been developed that have little sensitivity to the jet energy scale uncertainty. These include the measurement of the top mass using the following techniques: Fitting of the lepton p_T spectrum of candidate events [67]; Fitting of the transverse decay length of the b -jet (L_{xy}) [68]; Fitting the

invariant mass of a lepton from the W -decay and a muon from the semileptonic b decay [69].

Several measurements have now been made in which the top mass is extracted from the measured cross section using the theoretical relationship between the mass and the production cross section. This allows an extraction of both the pole and $\overline{\text{MS}}$ mass [70]. The direct measurements of the top mass, such as those shown in Table 2, are generally assumed to be measurements of the pole mass. Strictly speaking, the mass measured in these direct measurements is the mass used in the Monte Carlo generators, but the relation between the Monte Carlo generator mass and the pole mass is uncertain at the level of 1 GeV [71], which is now comparable to the measurement uncertainty.

Current global fits performed within the SM or its minimal supersymmetric extension, in which the top-mass measurements play a crucial role, provide indications for a relatively light Higgs (see “ H^0 Indirect Mass Limits” in the Particle Listings of this *Review* for more information). Such fits, including Z -pole data [77] and direct measurements of the mass and width of the W -boson, yield a pole top mass $m_t = 179_{-9}^{+12}$ GeV/ c^2 [78]. A fit including additional electroweak precision data (see the review “Electroweak Model and Constraints on New Physics” in this *Review*) yields $m_t = 177.5_{-7.8}^{+9.4}$ GeV/ c^2 . Both indirect evaluations are in good agreement with the direct top quark mass measurements. A review of top quark mass measurements can be found in reference [79].

C.2.2 Top Quark Spin Correlations and Width: One of the unique features of the top quark is that it typically decays before its spin can be depolarized by the strong interaction. Thus the top quark polarisation is directly observable via the angular distribution of its decay products. Hence, it is possible to define and measure observables sensitive to the top quark spin and its production mechanism. Although the top and antitop quarks are produced in strong interactions essentially unpolarized in hadron collisions, the spins of t and \bar{t} are correlated. For QCD processes, the $t\bar{t}$ system is dominantly produced in a 3S_1 state with parallel spins for $q\bar{q}$ annihilation

Table 2: Measurements of top quark mass from Tevatron and LHC. $\int \mathcal{L} dt$ is given in fb^{-1} . The results shown are mostly preliminary (not yet submitted for publication as of December 2011); for a complete set of published results see the Listings. Statistical uncertainties are listed first, followed by systematic uncertainties.

m_t (GeV/ c^2)	Source	$\int \mathcal{L} dt$	Ref. Channel
$175.1 \pm 0.8 \pm 1.3$	DØ Run I+II	≤ 5.4	[72] ℓ +jets + $\ell\ell$
$172.5 \pm 1.4 \pm 1.5$	CDF Run II	5.8	[65] All jets
$172.3 \pm 2.4 \pm 1.0$	CDF Run II	5.7	[66] Missing E_T +jets
$172.3 \pm 3.4 \pm 2.1$	CDF Run II	2.0	[64] $\ell\ell$
$172.7 \pm 9.3 \pm 3.7$	CDF Run II	2.2	[73] τ +jets
$172.7 \pm 0.6 \pm 0.9$	CDF Run I+II	≤ 5.8	[74] Multiple channels
$173.4 \pm 1.9 \pm 2.7$	CMS	0.036	[75] ℓ +jets + $\ell\ell$
$175.9 \pm 0.9 \pm 2.7$	ATLAS	0.70	[53] ℓ +jets
$173.5 \pm 0.6 \pm 0.8^*$	CDF,DØ CMS		publ. results, PDG best
$173.2 \pm 0.6 \pm 0.8^{**}$	CDF,DØ (I+II) ≤ 5.8		[76] publ. or prelim. results

* PDG uses this result as its best value. It is a combination of published measurements. See Listings for more details.

**The TEVEWWG world average is a combination of published Run 1 and preliminary or pub. Run-II meas., yielding a χ^2 of 8.3 for 11 deg. of freedom.

or in a 1S_0 state with antiparallel spins for gluon-gluon fusion. Hence, the situation at the Tevatron and at the LHC are complementary. The sensitivity to top spin is greatest when the top quark daughters are down-type fermions (charged leptons or d -type quarks), in which case the joint angular distribution is [80–82]

$$\frac{1}{\sigma} \frac{d^2\sigma}{d(\cos\theta_+)d(\cos\theta_-)} = \frac{1 + \kappa \cdot \cos\theta_+ \cdot \cos\theta_-}{4}, \quad (2)$$

where θ_+ and θ_- are the angles of the daughters in the top rest frames with respect to a particular spin quantization axis. The

maximum value for κ , 0.782 at NLO at the Tevatron [83], is found in the off-diagonal basis [80] while at the LHC the value at NLO is 0.326 in the helicity basis [83]. The spin correlation could be modified by a new production mechanism such as Z' bosons, Kaluza-Klein gluons or the Higgs boson.

CDF uses 5.1 fb^{-1} in the dilepton channel to measure the correlation coefficient in the beam axis [84]. They use the expected distributions of $(\cos\theta_+, \cos\theta_-)$ and $(\cos\theta_b, \cos\theta_{\bar{b}})$ of the charged leptons or the b -quarks in the $t\bar{t}$ signal and background templates to calculate a likelihood of observed reconstructed distributions as a function of assumed κ . They determine the 68% confidence interval for the correlation coefficient κ as $-0.52 < \kappa < 0.61$ or $\kappa = 0.04 \pm 0.56$ assuming $m_t = 172.5 \text{ GeV}/c^2$.

CDF also analyzes lepton+jets events in 5.3 fb^{-1} [85] assuming $m_t = 172.5 \text{ GeV}/c^2$. They form three separate templates - the same-spin template, the opposite-spin template, and the background template for the 2-dimensional distributions in $\cos(\theta_l)\cos(\theta_d)$ vs. $\cos(\theta_l)\cos(\theta_b)$. The fit to the data in the helicity basis returns an opposite helicity fraction of $F_{OH} = 0.74 \pm 0.24(\text{stat}) \pm 0.11(\text{syst})$. Converting this to the spin correlation coefficient yields $\kappa_{\text{helicity}} = 0.48 \pm 0.48(\text{stat}) \pm 0.22(\text{syst})$. In the beamline basis, they find an opposite spin fraction of $F_{OS} = 0.86 \pm 0.32(\text{stat}) \pm 0.13(\text{syst})$ which can be converted into a correlation coefficient of $\kappa_{\text{beam}} = 0.72 \pm 0.64(\text{stat}) \pm 0.26(\text{syst})$.

DØ performs a measurement of the ratio f of events with correlated t and \bar{t} spins to the total number of $t\bar{t}$ events in 5.3 fb^{-1} in the l+jets channel using a matrix element technique [86]. From 729 events they obtain $f_{\text{meas}} = 1.15_{-0.43}^{+0.42}$ (stat + syst) and can exclude values of $f < 0.420$ at the 95% C.L. In the dilepton channel [87], they also use a matrix element method and can exclude the hypothesis that the spins of the $t\bar{t}$ are uncorrelated at the 97.7% C.L.. The combination [86] yields $f_{\text{meas}} = 0.85 \pm 0.29$ (stat + syst) and a $t\bar{t}$ production cross section which is in good agreement with the SM prediction and previous measurements. For an expected fraction of $f = 1$, they can exclude $f < 0.481$ at the 95% C.L. For the observed value of $f_{\text{meas}} = 0.85$, they can exclude $f < 0.344(0.052)$ at

the 95(99.7)% C.L. The observed fraction f_{meas} translates to a measured asymmetry value of $A_{meas} = 0.66 \pm 0.23$ (stat + syst). They therefore obtain first evidence of SM spin correlation at 3.1 standard deviations.

Using 5.4 fb^{-1} of data, $D\bar{O}$ measures the correlation in the dilepton channel also from the angles of the two leptons in the t and \bar{t} rest frames, yielding a correlation strength $C = 0.10 \pm 0.45$ [88], in agreement with the NLO QCD prediction, but also in agreement with the no correlation hypothesis.

The ATLAS collaboration has performed a study of spin correlation in $t\bar{t}$ production at $\sqrt{s} = 7 \text{ TeV}$ using 0.70 fb^{-1} of data. Candidate events are selected in the dilepton topology with large missing transverse energy and at least two jets. The difference in azimuthal angle between the two charged leptons is compared to the expected distributions in the Standard Model, and to the case where the top quarks are produced with uncorrelated spin. Using the helicity basis as the quantisation axis, the strength of the spin correlation between the top and antitop quark is measured to be $A_{helicity} = 0.34_{-0.11}^{+0.15}$ [89], which is in agreement with the NLO Standard Model prediction.

Related to the measurement of top-spin correlations, which requires a top lifetime less than the hadronization timescale, is the measurement of the top width. The top width is expected to be of order $1 \text{ GeV}/c^2$ (Eq. 1). The sensitivity of current experiments does not approach this level in direct measurements.

CDF presents a measurement of the top quark width in the lepton+jets decay channel of $t\bar{t}$ events from a data sample corresponding to 4.3 fb^{-1} of integrated luminosity, yielding 756 events. The top quark mass and the mass of the hadronically decaying W boson that comes from the top quark decay are reconstructed for each event and compared with templates of different top quark widths (Γ_t) and deviations from nominal jet energy scale (ΔJES) to perform a simultaneous fit for both parameters, where ΔJES is used for the in situ calibration of the jet energy scale. By applying a Feldman-Cousins approach, they establish an upper limit at 95% C.L. of $\Gamma_t < 7.6 \text{ GeV}$ and a two-sided 68% C.L. interval of $0.3 \text{ GeV} < \Gamma_t < 4.4 \text{ GeV}$ [90], consistent with the Standard Model prediction.

DØ extracts the total width of the top quark from the partial decay width $\Gamma(t \rightarrow Wb)$ and the branching fraction $B(t \rightarrow Wb)$. $\Gamma(t \rightarrow Wb)$ is obtained from the measured t -channel cross section for single top quark production in 2.3 fb^{-1} , and $B(t \rightarrow Wb)$ is extracted from a measurement of the ratio $R = B(t \rightarrow Wb)/B(t \rightarrow Wq)$ in $\bar{t}t$ events in lepton+jets channels with 0, 1 and 2 b-tags in 1 fb^{-1} of integrated luminosity. Assuming $B(t \rightarrow Wq) = 1$, where q includes any kinematically accessible quark, the result is: $\Gamma_t = 1.99_{-0.55}^{+0.69} \text{ GeV}$ which translates to a top quark lifetime of $\tau_t = (3.3_{-0.9}^{+1.3}) \times 10^{-25} \text{ s}$. Assuming a high mass fourth generation b' quark and unitarity of the four-generation quark-mixing matrix, they set the first upper limit on $|V_{tb'}| < 0.63$ at 95% C.L. [91].

C.2.3 W Boson Helicity in Top Quark Decay: The Standard Model dictates that the top quark has the same vector-minus-axial-vector ($V - A$) charged-current weak interactions $\left(-i \frac{g}{\sqrt{2}} V_{tb} \gamma^\mu \frac{1}{2} (1 - \gamma_5)\right)$ as all the other fermions. In the SM, the fraction of top quark decays to longitudinally polarized W bosons is similar to its Yukawa coupling and hence enhanced with respect to the weak coupling. It is expected to be [92] $\mathcal{F}_0^{\text{SM}} \approx x/(1+x)$, $x = m_t^2/2M_W^2$ ($\mathcal{F}_0^{\text{SM}} \sim 70\%$ for $m_t = 175 \text{ GeV}/c^2$). Fractions of left-handed, right-handed, or longitudinal W bosons are denoted as \mathcal{F}_- , \mathcal{F}_+ , and \mathcal{F}_0 respectively. In the SM, \mathcal{F}_- is expected to be $\approx 30\%$ and $\mathcal{F}_+ \approx 0\%$.

The Tevatron and the LHC experiments use various techniques to measure the helicity of the W boson in top quark decays, in both the lepton+jets events and dilepton channels.

The first method uses a kinematic fit, similar to that used in the lepton+jets mass analyses, but with the top quark mass constrained to a fixed value, to improve the reconstruction of final-state observables, and render the under-constrained dilepton channel solvable. The distribution of the helicity angle ($\cos\theta^*$) between the lepton and the b quark in the W rest frame provides the most direct measure of the W helicity. In a simplified version of this approach, the $\cos\theta^*$ distribution is reduced to a forward-backward asymmetry.

The second method (p_T^ℓ) uses the different lepton p_T spectra from longitudinally or transversely polarized W -decays to determine the relative contributions.

A third method uses the invariant mass of the lepton and the b -quark in top decays ($M_{\ell b}^2$) as an observable, which is directly related to $\cos\theta^*$.

At the LHC, top quark pairs in the dilepton channels are reconstructed by solving a set of six independent kinematic equations on the missing transverse energy in x - and in y -direction, two W -masses, and the two top/antitop quark masses. In addition, the two jets with the largest p_T in the event are interpreted as b -jets. The pairing of the jets to the charged leptons is based on the minimisation of the sum of invariant masses m_{min} . Simulations show that this criterion gives the correct pairing in 68% of the events.

Finally, the Matrix Element method (ME) has also been used, in which a likelihood is formed from a product of event probabilities calculated from the ME for a given set of measured kinematic variables and assumed W -helicity fractions. The results of recent CDF, DØ and ATLAS analyses are summarized in Table 3.

The datasets are now large enough to allow for a simultaneous fit of \mathcal{F}_0 and \mathcal{F}_+ , which we denote by ‘2-param’ in the table. Results with either \mathcal{F}_0 or \mathcal{F}_+ fixed at its SM value are denoted ‘1-param’. For the simultaneous fits the correlation coefficient between the two values is about -0.8 for both experiments. A complete set of published results can be found in the Listings. All results are in agreement with the SM expectation.

C.2.4 Top Quark Electric Charge: The top quark is the only quark whose electric charge has not been measured through production at threshold in e^+e^- collisions. Furthermore, it is the only quark whose electromagnetic coupling has not been observed and studied until recently. Since the CDF and DØ analyses on top quark production did not associate the b , \bar{b} , and W^\pm uniquely to the top or antitop, decays such as $t \rightarrow W^+\bar{b}$, $\bar{t} \rightarrow W^-b$ were not excluded. A charge $4/3$ quark of this kind is consistent with current electroweak precision data. The $Z \rightarrow \ell^+\ell^-$ and $Z \rightarrow b\bar{b}$ data, in particular the discrepancy

Table 3: Measurement and 95% C.L. upper limits of the W helicity in top quark decays. Most results listed are preliminary and not yet submitted for publication, as of December 2011. A full set of published results is given in the Listings.

W Helicity	Source	$\int \mathcal{L} dt$ (fb $^{-1}$)	Ref.	Method
$\mathcal{F}_0 = 0.71 \pm 0.20$	CDF Run II	5.3	[93]	$\cos \theta^*$ 2-param
$\mathcal{F}_0 = 0.59 \pm 0.11$	CDF Run II	5.3	[93]	$\cos \theta^*$ 1-param
$\mathcal{F}_0 = 0.65 \pm 0.19$	CDF Run II	1.9	[94]	$\cos \theta^*$ 2-param
$\mathcal{F}_0 = 0.59 \pm 0.12$	CDF Run II	1.9	[94]	$\cos \theta^*$ 1-param
$\mathcal{F}_0 = 0.67 \pm 0.13$	DØ Run II	5.4	[95]	$\cos \theta^*$ 2-param
$\mathcal{F}_0 = 0.73 \pm 0.08$	CDF+DØ Run II	5.4	[96]	$\cos \theta^*$ 2-param
$\mathcal{F}_0 = 0.69 \pm 0.06$	CDF+DØ Run II	5.4	[96]	$\cos \theta^*$ 1-param
$\mathcal{F}_0 = 0.57 \pm 0.11$	ATLAS	0.7	[97]	$\cos \theta^*$ 3-param
$\mathcal{F}_0 = 0.75 \pm 0.08$	ATLAS	0.7	[97]	$\cos \theta^*$, m_{min} 2-param
$\mathcal{F}_+ = -0.07 \pm 0.10$	CDF Run II	5.3	[93]	$\cos \theta^*$ 2-param
$\mathcal{F}_+ = -0.07 \pm 0.05$	CDF Run II	5.3	[93]	$\cos \theta^*$ 1-param
$\mathcal{F}_+ = -0.03 \pm 0.08$	CDF Run II	1.9	[94]	$\cos \theta^*$ 2-param
$\mathcal{F}_+ = -0.04 \pm 0.05$	CDF Run II	1.9	[94]	$\cos \theta^*$ 1-param
$\mathcal{F}_+ = 0.02 \pm 0.05$	DØ Run II	5.4	[95]	$\cos \theta^*$ 2-param
$\mathcal{F}_+ = -0.04 \pm 0.05$	CDF+DØ Run II	5.4	[96]	$\cos \theta^*$ 2-param
$\mathcal{F}_+ = -0.01 \pm 0.04$	CDF+DØ Run II	5.4	[96]	$\cos \theta^*$ 1-param
$\mathcal{F}_+ = 0.09 \pm 0.09$	ATLAS	0.7	[97]	$\cos \theta^*$ 3-param

between A_{LR} from SLC at SLAC and $A_{FB}^{0,b}$ of b -quarks and $A_{FB}^{0,\ell}$ of leptons from LEP at CERN, can be fitted with a top quark of mass $m_t = 270$ GeV/ c^2 , provided that the right-handed b quark mixes with the isospin $+1/2$ component of an exotic doublet of charge $-1/3$ and $-4/3$ quarks, $(Q_1, Q_4)_R$ [98,99].

DØ studies the top quark charge in double-tagged lepton+jets events, CDF does it in single-tagged lepton+jets and dilepton events. Assuming the top and antitop quarks have equal but opposite electric charge, then reconstructing the charge of the b -quark through jet charge discrimination techniques, the $|Q_{top}| = 4/3$ and $|Q_{top}| = 2/3$ scenarios can be

differentiated. For the exotic model of Chang *et al.* [99] with a top quark charge $|Q_{top}| = 4/3$, DØ excludes the exotic model at 91.2% C.L.% [100] using 370 pb^{-1} , while CDF excludes the model at 99% C.L. [101] in 5.6 fb^{-1} . Both results indicate that the observed particle is indeed consistent with being a SM $|Q_{top}| = 2/3$ quark. In 0.70 fb^{-1} , ATLAS performed a similar analysis, reconstructing the b -quark charge either via a jet-charge technique or via the lepton charge in soft muon decays in combination with a kinematic likelihood fit. They exclude the exotic scenario at more than 5σ [102].

The electromagnetic or the weak coupling of the top quark can be probed directly by investigating $t\bar{t}$ events with an additional gauge boson, like $t\bar{t}\gamma$ and $t\bar{t}Z$ events. Top quark pair events with additional photons in the final state are directly sensitive to the $t\bar{t}\gamma$ vertex.

CDF performs a search for events containing a lepton, a photon, significant missing transverse momentum, and a jet identified as containing a b -quark and at least three jets and large total transverse energy in 1.9 fb^{-1} . They find 16 $t\bar{t}\gamma$ events with an expectation from SM sources of $11.2^{+2.3}_{-2.1}$ events which they translate into a measurement of the $t\bar{t}\gamma$ cross section measurement of $0.15 \pm 0.08 \text{ pb}$ [103]. Recently, CDF repeated this measurement with 6.0 fb^{-1} and reported evidence for the observation of $t\bar{t}\gamma$ production with a cross section $\sigma_{t\bar{t}\gamma} = 0.18 \pm 0.08 \text{ pb}$ and a ratio of $\sigma_{t\bar{t}\gamma}/\sigma_{t\bar{t}} = 0.024 \pm 0.009$ [104].

ATLAS performed a first measurement of the $t\bar{t}\gamma$ cross section in pp collisions at $\sqrt{s} = 7 \text{ TeV}$ using 1.04 fb^{-1} of data. Events are selected that contain a large transverse momentum electron or muon and a large transverse momentum photon, yielding 52 and 70 events in the electron and muon samples, respectively. The resulting cross section times branching ratio into the single lepton and dilepton channels for $t\bar{t}\gamma$ production with a photon with transverse momentum above 8 GeV is $\sigma(t\bar{t}\gamma) = 2.0 \pm 0.5(stat.) \pm 0.7(syst.) \pm 0.1(lumi.) \text{ pb}$ [105], which is consistent with theoretical calculations. A real test, however, of the vector and axial vector couplings in $t\bar{t}\gamma$ events or searches for possible tensor couplings of top quarks to photons

will only be feasible with an integrated luminosity of several fb^{-1} in the future.

C.3 Searches for Non-Standard Model Top Quark Production & Decay:

Motivated by the large mass of the top quark, several models suggest that the top quark plays a role in the dynamics of electroweak symmetry breaking. One example is topcolor [106], where a large top quark mass can be generated through the formation of a dynamic $t\bar{t}$ condensate, X , which is formed by a new strong gauge force coupling preferentially to the third generation. Another example is topcolor-assisted technicolor [107], predicting a heavy Z' boson that couples preferentially to the third generation of quarks with cross sections expected to be visible at the Tevatron and the LHC. CDF, DØ, ATLAS, and CMS have searched for $t\bar{t}$ production via intermediate, narrow-width, heavy-vector bosons X in the lepton+jets, the dilepton or the all-jets channels.

CDF has searched for resonant production of $t\bar{t}$ pairs in 4.8 fb^{-1} of data in the lepton+jets channel. A matrix element reconstruction technique is used; for each event a probability density function (pdf) of the $t\bar{t}$ candidate invariant mass is sampled. These pdfs are used to construct a likelihood function, whereby the cross section for resonant $t\bar{t}$ production is estimated, given a hypothetical resonance mass and width. The data indicate no evidence of resonant production of $t\bar{t}$ pairs. A benchmark model of leptophobic $Z \rightarrow t\bar{t}$ is excluded with $m_{Z'} < 900 \text{ GeV}$ at 95% C.L. [108]. A similar analysis has been performed in the all-jets channel using 2.8 fb^{-1} of data [109]. In the absence of any evidence for top-antitop quark resonant production upper limits on the production cross section times branching ratio for a specific topcolor assisted technicolor model with width of $\Gamma_{Z'} = 0.012M_{Z'}$ are set. Within this model, they exclude Z' bosons with masses below 805 GeV at the 95% C.L.

DØ has searched for narrow $t\bar{t}$ resonances that decay into a lepton+jets final state based on 5.3 fb^{-1} . They place upper limits on the production cross section times branching fraction to $t\bar{t}$ in comparison to the prediction for a leptophobic topcolor Z' boson. They exclude such a resonance at the 95% C.L.

for masses below 835 GeV at width $\Gamma_{Z'} = 0.012M_{Z'}$ [110]. This limit turns out to be independent of couplings of the $t\bar{t}$ resonance (pure vector, pure axial-vector, or Standard Model Z-like) and is valid for any narrow resonance decaying 100% to a $t\bar{t}$ final state.

ATLAS has performed a search for $t\bar{t}$ resonances in the lepton+jets final states using 0.2 fb^{-1} of data at $\sqrt{s} = 7 \text{ TeV}$. No evidence for a resonance is found. Using the reconstructed $t\bar{t}$ mass spectrum, limits are set on the production cross-section times branching ratio to $t\bar{t}$ for narrow and wide resonances. For narrow Z' models, the observed 95% C.L. limits range from approximately 38 pb to 3.2 pb for masses going from $m_{Z'} = 500 \text{ GeV}$ to $m_{Z'} = 1300 \text{ GeV}$ [111]. In Randall-Sundrum models, Kaluza-Klein gluons with masses below 650 GeV are excluded at 95% C.L. Using 1.04 fb^{-1} of data in the dilepton channel, they have not observed any significant excess and place upper limits at the 95% C.L. on the cross section times branching ratio of the resonance decaying to $t\bar{t}$ pairs as a function of the resonance pole mass. A lower mass limit of 0.84 TeV is set for the case of a Kaluza Klein gluon resonance in the Randall-Sundrum Model [112].

CMS performs a search for massive neutral bosons decaying via a top-antitop quark pair. The analysis is based on 36 pb^{-1} of data. From a combined analysis of the muon plus jets and electron plus jets decay modes no significant signal is observed, and upper limits on the production cross section as a function of the boson mass are reported [113]. They also perform a search for narrow heavy resonances decaying to top quark pairs in the μ +jets channel using 1.1 fb^{-1} and set sub-picobarn limits at 95% C.L. on $\sigma(pp \rightarrow Z' \rightarrow t\bar{t})$ for invariant Z' masses above $1.35 \text{ TeV}/c^2$ [114]. Using 0.9 fb^{-1} , they search in the all-hadronic channel for sufficiently heavy resonances with decay products partially or fully merged into one jet. They set sub-picobarn limits on $\sigma_{Z'} \times B(Z' \rightarrow t\bar{t})$ at 95% C.L. for Z' heavier than $1.1 \text{ TeV}/c^2$ [115].

Both CDF and DØ have searched for non-SM top decays [116–121], particularly those expected in supersymmetric models, such as $t \rightarrow H^+b$, followed by $H^+ \rightarrow \tau^+\bar{\nu}$

or $c\bar{s}$. The $t \rightarrow H^+b$ branching ratio has a minimum at $\tan\beta = \sqrt{m_t/m_b} \simeq 6$, and is large in the region of either $\tan\beta \ll 6$ or $\tan\beta \gg 6$. In the former range, $H^+ \rightarrow c\bar{s}$ is dominant, while $H^+ \rightarrow \tau^+\bar{\nu}$ dominates in the latter range. These studies are based either on direct searches for these final states, or on top “disappearance.” In the standard lepton+jets or dilepton cross-section analyses, any charged-Higgs decays are not detected as efficiently as $t \rightarrow W^\pm b$, primarily because the selection criteria are optimized for the standard decays, and because of the absence of energetic isolated leptons in Higgs decays. A significant $t \rightarrow H^+b$ contribution would give rise to measured $t\bar{t}$ cross sections that would be lower than the prediction from the SM (assuming that non-SM contributions to $t\bar{t}$ production are negligible), and the measured cross-section ratio $\sigma_{t\bar{t}}^{\ell+jets}/\sigma_{t\bar{t}}^{\ell\ell}$ would differ from unity.

In Run II, CDF has searched for charged-Higgs production in dilepton, lepton+jets, and lepton+hadronic tau final states, considering possible H^+ decays to $c\bar{s}$, $\tau\bar{\nu}$, t^*b , or W^+h^0 , in addition to the SM decay $t \rightarrow W^+b$ [118,119]. Depending on the top and Higgs-decay branching ratios, which are scanned in a particular 2-Higgs doublet benchmark model, the number of expected events in these decay channels can show an excess or deficit when compared to SM expectations. A model-independent interpretation yields a limit of $B(t \rightarrow H^\pm b) < 0.91$ at 95% C.L. for $m_{H^\pm} \approx 100$ GeV, and $B(t \rightarrow H^\pm b) < 0.4$ in the tauonic model with $B(H^\pm \rightarrow \tau\nu) = 100\%$. In a more recent search, the dijet invariant mass in lepton+jets events has been used in 2.2 fb^{-1} to search for a charged Higgs decaying to $c\bar{s}$ with mass above the W boson mass. The absence of a signal leads to a 95% C.L. limit of $B(t \rightarrow H^\pm b) \times B(H^\pm \rightarrow c\bar{s}) < 0.1$ to 0.3 for masses between 90 and 150 GeV/ c^2 [119].

In 1 fb^{-1} of integrated luminosity, the DØ collaboration has used the $t\bar{t}$ dilepton and lepton+jets events, including τ lepton channels, to search for evidence of charged-Higgs decays into τ leptons via the ratio of events with τ leptons to those with e and μ [120], global fits [121] and topological searches [122]. They exclude regions of $B(t \rightarrow H^\pm b)$ as a function of Higgs mass, ranging from $B(t \rightarrow H^\pm b) > 0.12$ at low mass to

$B(t \rightarrow H^\pm b) > 0.2$ at high mass. In a companion analysis they look for evidence of leptophobic charged Higgs production in top decays in which the Higgs decays purely hadronically, leading to a suppression of the measured $t\bar{t}$ rate in all leptonic channels. They exclude $B(t \rightarrow H^\pm b) > 0.2$ for charged-Higgs masses between 80 and 155 GeV/c².

DØ combines measurements of the top quark pair production cross section in the ℓ +jets, $\ell\ell$, and $\tau\ell$ final states (where ℓ is an electron or muon) in 1 fb⁻¹ of data, yielding $\sigma_{t\bar{t}} = 8.18_{-0.87}^{+0.98}$ pb for $m_t = 170$ GeV, or based on QCD predictions extract a top quark mass consistent with the world average. In addition, they measure the cross section ratios to be $\sigma_{ll}/\sigma_{lj} = 0.86_{-0.17}^{+0.19}(\text{stat} + \text{syst})$ and $\sigma_{\tau l}/\sigma_{ll+j} = 0.97_{-0.29}^{+0.32}(\text{stat} + \text{syst})$. Based on this, they set upper limits on the branching fractions $B(t \rightarrow H^\pm b \rightarrow \tau^\pm \nu b)$ and $B(t \rightarrow H^\pm b \rightarrow c\bar{s}b)$ as a function of the charged Higgs boson mass [123].

In 35 pb⁻¹, ATLAS searches for the decay $H^\pm \rightarrow c\bar{s}$ in the lepton+jets channel by investigation of the invariant jj -mass spectrum. The observed limits are within one standard deviation of the expected limits and range from $B = 0.25$ to 0.14 for $m_{H^\pm} = 90$ to 130 GeV/c² [124]. In 1.03 fb⁻¹ ATLAS searches for $t\bar{t} \rightarrow \tau(\rightarrow \text{hadrons}) + \text{jets}$. They set a 95% C.L. limit on the production of branching ratios $B(t \rightarrow bH^\pm) \times B(H^\pm \rightarrow \tau\nu)$ of 0.03 to 0.10 for H^\pm masses in the range 90 GeV/c² < m_{H^\pm} < 160 GeV/c² [125]. A similar analysis with τ decaying to leptons in 1.03 fb⁻¹, assuming $B(H^\pm \rightarrow \tau\nu) = 1$, this leads to 95% C.L. upper limits on the branching fraction $B(t \rightarrow bH^\pm)$ between 5.2% and 14.1% for H^\pm masses in the range 90 GeV/c² < m_{H^\pm} < 160 GeV/c² [126].

The ATLAS collaboration has also searched for FCNC processes in 0.7 fb⁻¹ of $t\bar{t}$ events with one top quark decaying through FCNC ($t \rightarrow qZ$) and the other through the Standard Model dominant mode ($t \rightarrow bW$). Only the decays of the Z boson to charged leptons and leptonic W boson decays were considered as signal, leading to a final state topology characterised by the presence of three isolated leptons, at least two jets and missing transverse energy from the undetected

neutrino. No evidence for an FCNC signal was found. An upper limit on the $t \rightarrow qZ$ branching ratio of $B(t \rightarrow qZ) < 1.1\%$ is set at the 95% confidence level, compatible with the expected limit, assuming no FCNC decay, of $B(t \rightarrow qZ) < 1.3\%$ [127].

More details, and the results of these studies for the exclusion in the $m_{H^\pm}, \tan\beta$ plane, can be found in the review “Higgs Bosons: Theory and Searches” and in the “ H^+ Mass Limits” section of the Higgs Particle Listings of the current edition.

Using up to 2.7 fb^{-1} of data, DØ has measured the Wtb coupling form factors by combining information from the W boson helicity in top quark decays in $t\bar{t}$ events and single-top quark production, allowing to place limits on the left-handed and right-handed vector and tensor couplings [128–130].

In 2.3 fb^{-1} , DØ excludes the production of W' bosons with masses below $863 \text{ GeV}/c^2$ for a W' boson with Standard Model-like couplings, below $885 \text{ GeV}/c^2$ for a W' boson with right-handed couplings that is allowed to decay to both leptons and quarks, and below $890 \text{ GeV}/c^2$ for a W' boson with right-handed couplings that is only allowed to decay to quarks [131]. CDF has recently released W' limits also using the single-top analysis [132]. In 1.9 fb^{-1} of Run-II data, a W' with Standard Model couplings is searched for in the $t\bar{b}$ decay mode. Masses below $800 \text{ GeV}/c^2$ are excluded, assuming that any right-handed neutrino is lighter than the W' , and below $825 \text{ GeV}/c^2$ if the right-handed neutrino is heavier than the W' .

CDF reported a search for flavor-changing neutral-current (FCNC) decays of the top quark $t \rightarrow q\gamma$ and $t \rightarrow qZ$ in the Run-I data [133], and recently with enhanced sensitivity in Run II [134]. The SM predicts such small rates that any observation would be a sign of new physics. CDF assumes that one top decays via FCNC, while the other decays via Wb . The Run-I analysis included a $t \rightarrow q\gamma$ search in which two signatures are examined, depending on whether the W decays leptonically or hadronically. For leptonic W decay, the signature is $\gamma\ell$ and missing E_T and two or more jets, while for hadronic W decay, it is $\gamma+ \geq 4$ jets. In either case, one of the jets must have a secondary vertex b tag. One event is observed ($\mu\gamma$) with an expected background of less than half an event, giving an upper

limit on the top branching ratio of $B(t \rightarrow q\gamma) < 3.2\%$ at 95% C.L. In the search for $t \rightarrow qZ$, CDF considers $Z \rightarrow \mu\mu$ or ee and $W \rightarrow qq'$, giving a $Z +$ four jets signature. A Run-II dataset of 1.9 fb^{-1} is found consistent with background expectations and a 95% C.L. on the $t \rightarrow qZ$ branching fraction of $< 3.7\%$ (for $m_t = 175 \text{ GeV}/c^2$) is set [134]. By comparison to the number expected from the theoretical production cross section, CDF has used the observed number of double b -tagged lepton+jets candidate events to place limits on a variety of decay modes, ranging from $B(t \rightarrow Zc) < 13\%$ to $B(t \rightarrow \text{invisible}) < 9\%$ [135].

In 4.1 fb^{-1} , DØ performs a search for events with $t\bar{t} \rightarrow \ell'\nu\ell\bar{\ell} + \text{jets}$ ($\ell, \ell' = e, \mu$) and extracts limits on the branching ratio $B(t \rightarrow Zq)$ ($q = u, c$ quarks) $< 3.2\%$ at 95% C.L. [136]. DØ performs also in single-top event candidates with an additional jet searches for flavor changing neutral currents via quark-gluon couplings, using 2.3 fb^{-1} . They find consistency between background expectation and observed data and set cross section limits at the 95% C.L. of $\sigma_{tgu} < 0.20 \text{ pb}$ and $\sigma_{tgc} < 0.27 \text{ pb}$ which corresponds to limits on the top quark decay branching fractions of $B(t \rightarrow gu) < 2.0 \cdot 10^{-4}$ and $B(t \rightarrow gc) < 3.9 \cdot 10^{-3}$ [137].

Constraints on FCNC couplings of the top quark can also be obtained from searches for anomalous single-top production in e^+e^- collisions, via the process $e^+e^- \rightarrow \gamma, Z^* \rightarrow t\bar{q}$ and its charge-conjugate ($q = u, c$), or in $e^\pm p$ collisions, via the process $e^\pm u \rightarrow e^\pm t$. For a leptonic W decay, the topology is at least a high- p_T lepton, a high- p_T jet and missing E_T , while for a hadronic W -decay, the topology is three high- p_T jets. Limits on the cross section for this reaction have been obtained by the LEP collaborations [138] in e^+e^- collisions, and by H1 [139] and ZEUS [140] in $e^\pm p$ collisions. When interpreted in terms of branching ratios in top decay [141,142], the LEP limits lead to typical 95% C.L. upper bounds of $B(t \rightarrow qZ) < 0.137$. Assuming no coupling to the Z boson, the 95% C.L. limits on the anomalous FCNC coupling $\kappa_\gamma < 0.13$ and < 0.27 by ZEUS and H1, respectively, are stronger than the CDF limit of $\kappa_\gamma < 0.42$, and improve over LEP sensitivity in that domain. The H1 limit is slightly weaker than the ZEUS limit due to

an observed excess of five-candidate events over an expected background of 3.2 ± 0.4 . If this excess is attributed to FCNC top quark production, this leads to a total cross section of $\sigma(ep \rightarrow e + t + X, \sqrt{s} = 319 \text{ GeV}) < 0.25 \text{ pb}$ [139,143].

References

CDF note references can be retrieved from www-cdf.fnal.gov/physics/new/top/top.html, and DØ note references from www-d0.fnal.gov/Run2Physics/WWW/documents/Run2Results.htm and ATLAS note references from <https://twiki.cern.ch/twiki/bin/view/AtlasPublic/TopPublicResults> and CMS note references from <https://twiki.cern.ch/twiki/bin/view/CMSPublic/PhysicsResultsTOP>.

1. M. Cacciari *et al.*, JHEP **0809**, 127 (2008); N. Kidonakis and R. Vogt, Phys. Rev. **D78**, 074005 (2008); S. Moch and P. Uwer, Nucl. Phys. (Proc. Supp.) **B183**, 75 (2008).
2. S. Moch and P. Uwer, Phys. Rev. **D78**, 034003 (2008); M. Beneke *et al.* Phys. Lett. **B690**, 483 (2010); M. Beneke, P. Falgari, S. Klein and C. Schwinn, Nucl. Phys. **B855**, 695 (2012); V. Ahrens, M. Neubert, B. D. Pecjak, A. Ferroglia and L. L. Yang, Phys. Lett. **B703**, 135 (2011); M. Cacciari, M. Czakon, M. L. Mangano, A. Mitov and P. Nason, arXiv:1111.5869 [hep-ph] (2011).
3. U. Langenfeld, S. Moch, and P. Uwer, Phys. Rev. **D80**, 054009 (2009); U. Langenfeld, S. Moch, and P. Uwer, arXiv:0907.2527 [hep-ph] (2009).
4. M. Cacciari *et al.*, Sov. Phys. JETP **04**, 068 (2004).
5. M. Aliev *et al.* Comp. Phys. Comm. **182**, 10341046 (2011).
6. S. Cortese and R. Petronzio, Phys. Lett. **B253**, 494 (1991).
7. S. Willenbrock and D. Dicus, Phys. Rev. **D34**, 155 (1986).
8. N. Kidonakis, Phys. Rev. **D83**, 091503 (2011).
9. N. Kidonakis, Phys. Rev. **D81**, 054028 (2010).
10. N. Kidonakis, Phys. Rev. **D82**, 054018 (2010).
11. T. Tait and C.-P. Yuan. Phys. Rev. **D63**, 014018 (2001).
12. M. Jezabek and J.H. Kühn, Nucl. Phys. **B314**, 1 (1989).
13. I.I.Y. Bigi *et al.*, Phys. Lett. **B181**, 157 (1986).

14. A. Czarnecki and K. Melnikov, Nucl. Phys. **B544**, 520 (1999); K.G. Chetyrkin *et al.*, Phys. Rev. **D60**, 114015 (1999).
15. S. Frixione and B. Webber, hep-ph/0402116; S. Frixione and B. Webber, JHEP **06**, 029 (2002); S. Frixione, P. Nason and B. Webber, JHEP **08**, 007 (2003); S. Frixione, P. Nason and G. Ridolfi, hep-ph/07073088.
16. J.M. Campbell and R.K. Ellis, Phys. Rev. **D62**, 114012 (2000), Phys. Rev. **D65**, 113007 (2002); J.M. Campbell and J. Huston, Phys. Rev. **D70**, 094021 (2004); J. Campbell and M. Mangano, Ann. Rev. Nucl. and Part. Sci. **61**, 311 (2011).
17. V.M. Abazov *et al.* (DØ Collab.), Phys. Lett. **B704**, 403 (2011).
18. T. Aaltonen *et al.* (CDF Collab.), CDF conference note 9913 (2009).
19. ATLAS Collab., ATLAS-CONF-2011-108.
20. ATLAS Collab., ATLAS-CONF-2011-121.
21. ATLAS Collab., ATLAS-CONF-2011-140.
22. CMS Collab., CMS-PAS-TOP-11-003.
23. CMS Collab., CMS-PAS-TOP-11-007.
24. V.M. Abazov *et al.* (DØ Collab.) Phys. Rev. Lett. **107**, 121802, (2011); D. Acosta *et al.* (CDF Collab.) Phys. Rev. Lett. **95**, 102002, (2005).
25. V.M. Abazov *et al.* (DØ Collab.), Phys. Rev. **D67**, 012004 (2003).
26. T. Affolder *et al.* (CDF Collab.), Phys. Rev. **D64**, 032002 (2001).
27. M. Czakon and A. Mitov, Nucl. Phys. **B824**, 111 (2010).
28. V.M. Abazov *et al.* (DØ Collab.), Phys. Rev. Lett. **103**, 092001 (2009); V.M. Abazov *et al.* (DØ Collab.), Phys. Rev. **D78**, 12005 (2008); V.M. Abazov *et al.* (DØ Collab.), Phys. Rev. Lett. **98**, 181802 (2007).
29. T. Aaltonen *et al.* (CDF Collab.), Phys. Rev. Lett. **103**, 092002 (2009); T. Aaltonen *et al.* (CDF Collab.), Phys. Rev. **D81**, 072003 (2010).
30. T. Aaltonen *et al.* (CDF Collab.), Phys. Rev. **D82**, 112005 (2010).
31. A. Heinson and T. Junk, Ann. Rev. Nucl. Part. Sci. **61**, 171 (2011).
32. Tevatron Electroweak Working Group, arXiv:0908.2171v1 [hep-ex].

33. V.A. Abazov *et al.* (DØ Collab.), Phys. Rev. **D84**, 112001 (2001).
34. CDF Collab., CDF conference note 9712 (2009).
35. V.M. Abazov *et al.* (DØ Collab.), Phys. Lett. **B705**, 313 (2011).
36. ATLAS Collab., ATLAS-CONF-2011-101.
37. CMS Collab., Phys. Rev. Lett. **107**, 091802 (2011).
38. C.D. White *et al.*, JHEP **11**, 74 (2009).
39. S. Frixione *et al.*, JHEP **07**, 29 (2008).
40. ATLAS Collab., ATLAS-CONF-2011-104.
41. CMS Collab., CMS-PAS-TOP-11-022.
42. O. Antunano, J.H. Kühn and G. Rodrigo, Phys. Rev. **D77**, 014003 (2008); M.T. Bowen, S. Ellis and D. Rainwater, Phys. Rev. **D73**, 014008 (2006); S. Dittmaier, P. Uwer and S. Weinzierl, Phys. Rev. Lett. **98**, 262002 (2007); L.G. Almeida, G. Sterman, and W. Vogelsang, Phys. Rev. **D78**, 014008 (2008).
43. S. Jung, H. Murayama, A. Pierce, J.D. Wells, Phys. Rev. **D81**, 015004 (2010).
44. V.M. Abazov *et al.* (DØ Collab.), Phys. Rev. Lett. **100**, 142002 (2008).
45. T. Aaltonen *et al.* (CDF Collab.), Phys. Rev. Lett. **101**, 202001 (2008).
46. V.M. Abazov *et al.* (DØ Collab.), Phys. Rev. **D84**, 112005 (2011).
47. CDF Collab., CDF conference note 10584 (2011).
48. T. Aaltonen, *et al.* (CDF Collab.), Phys. Rev. **D83**, 112003 (2011).
49. CMS Collab., CMS-PAS-TOP-11-014,.
50. ATLAS Collab., ATL-CONF-2011-106.
51. F. Abe *et al.* (CDF Collab.), Phys. Rev. **D50**, 2966 (1994).
52. A. Abulencia *et al.* (CDF Collab.), Phys. Rev. **D73**, 032003 (2006).
53. ATLAS Collab., ATLAS-CONF-2011-120.
54. T. Aaltonen *et al.* (CDF Collab.), Phys. Rev. **D83**, 111101 (R)(2011).
55. V.M. Abazov *et al.* (DØ Collab.), Nature, **429**, 638 (2004).
56. K. Kondo *et al.* J. Phys. Soc. Jpn. **G62**, 1177 (1993).

57. R.H. Dalitz and G.R. Goldstein, Phys. Rev. **D45**, 1531 (1992); Phys. Lett. **B287**, 225 (1992); Proc. Royal Soc. London **A445**, 2803 (1999).
58. V.M. Abazov *et al.* (DØ Collab.), Phys. Rev. **D84**, 032004 (2011).
59. V.M. Abazov *et al.* (DØ Collab.), Phys. Rev. **D75**, 092001 (2007).
60. L. Sonnenschein, Phys. Rev. **D73**, 054015 (2006).
61. A. Abulencia *et al.* (CDF Collab.), Phys. Rev. **D74**, 032009 (2006).
62. V.M. Abazov *et al.* (DØ Collab.), Phys. Rev. Lett. **107**, 082004 (2011).
63. B. Abbot *et al.* (DØ Collab.), Phys. Rev. **D60**, 052001 (1999); F. Abe *et al.* (CDF Collab.), Phys. Rev. Lett. **82**, 271 (1999).
64. CDF Collab., CDF conference note 10635 (2011).
65. CDF Collab., CDF conference note 10456 (2011), [arXiv:1112.4891](#).
66. T.Aaltonen *et al.* (CDF Collab.), Phys. Rev. Lett. **107**, 232002 (2011).
67. T.Aaltonen *et al.* (CDF Collab.), Phys. Lett. **B698**, 371 (2011).
68. T. Aaltonen *et al.* (CDF Collab.), Phys. Rev. **D81**, 032002, (2010).
69. T. Aaltonen *et al.* (CDF Collab.), Phys. Rev. **D80**, 051104, (2009).
70. V.M. Abazov *et al.* (DØ Collab.) Phys. Rev. Lett. **100**, 192004, (2008);
V.M. Abazov *et al.* (DØ Collab.) Phys. Lett. **B703**, 422, (2011);
ATLAS Collab., ATLAS-CONF-2011-054;
CMS Collab., CMS-PAS-TOP-11-008;
U.Langefeld, S.Moch, P.Uwer, Phys. Rev. **D80**, 054009 (2009).
71. A.H. Hoang and J.W. Stewart, Nucl. Phys. Proc. Suppl. **185**, 220 (2008).
72. DØ Collab., DØ conference note 6189 (2011).
73. CDF Collab., CDF conference note 10562 (2011).
74. CDF Collab., CDF conference note 10444 (2011).
75. CMS Collab., CMS-PAS-TOP-10-009.
76. The Tevatron Electroweak Working Group, For the CDF and DØ Collaborations, [arXiv:1107.5255v3](#).

77. ALEPH, DELPHI, L3, OPAL, SLD and Working Groups, Phys. Reports **427**, 257 (2006).
78. The LEP Collaborations: ALEPH, DELPHI, L3, OPAL, SLD, CDF, and DØ Collaborations, and the LEP, Tevatron and SLD Electroweak Working Groups, [arXiv:1012.2367v2](https://arxiv.org/abs/1012.2367v2).
79. A. B. Galtieri, F. Margaroli, I. Volobouev, Rept. on Prog. in Phys. **75**, 056201 (2012).
80. G. Mahlon and S. Parke, Phys. Rev. **D53**, 4886 (1996); G. Mahlon and S. Parke, Phys. Lett. **B411**, 173 (1997).
81. G.R. Goldstein, in *Spin 96: Proceedings of the 12th International Symposium on High Energy Spin Physics*, Amsterdam, 1996, ed. C.W. Jager (World Scientific, Singapore, 1997), p. 328.
82. T. Stelzer and S. Willenbrock, Phys. Lett. **B374**, 169 (1996).
83. W. Bernreuther *et al.* Nucl. Phys. **B690**, 81 (2004).
84. CDF Collab., CDF conference note 10719 (2011).
85. CDF Collab., CDF conference note 10211 (2010).
86. V.M. Abazov *et al.* (DØ Collab.) [arXiv:1110.4194](https://arxiv.org/abs/1110.4194), to be published in Phys. Rev. Lett.
87. V.M. Abazov *et al.* (DØ Collab.), Phys. Rev. Lett. **107**, 032001 (2011).
88. V.M. Abazov *et al.* (DØ Collab.), Phys. Lett. **B702**, 16 (2011).
89. ATLAS Collab., ATLAS-CONF-2011-117.
90. T. Aaltonen *et al.* (CDF Collab.) Phys. Rev. Lett. **105**, 232003 (2010).
91. V.M. Abazov *et al.* (DØ Collab.) Phys. Rev. Lett. **106**, 02201 (2011).
92. G.L. Kane, G.A. Ladinsky, and C.P. Yuan, Phys. Rev. **D45**, 124 (1992).
93. CDF Collab., CDF conference note 10543 (2011).
94. CDF Collab., CDF conference note 9215 (2007).
95. V.M. Abazov *et al.* (DØ Collab.), Phys. Rev. **D83**, 032009 (2011).
96. CDF Collab., CDF conference note 10622 (2011); DØ Collab., DØ conference note 6231 (2011).
97. ATLAS Collab., ATLAS-CONF-2011-122.
98. D. Choudhury, T.M.P. Tait, and C.E.M. Wagner, Phys. Rev. **D65**, 053002 (2002).

99. D. Chang, W.F. Chang, and E. Ma, Phys. Rev. **D59**, 091503 (1999), Phys. Rev. **D61**, 037301 (2000).
100. V.M. Abazov *et al.* (DØ Collab.), Phys. Rev. Lett. **98**, 041801 (2007).
101. CDF Collab., CDF conference note 10460 (2011).
102. ATLAS Collab., ATLAS-CONF-2011-141.
103. T. Aaltonen *et al.* (CDF Collab.), Phys. Rev. **D80**, 011102 (2009).
104. T. Aaltonen *et al.* (CDF Collab.), Phys. Rev. **D84**, 031104 (2011).
105. ATLAS Collab., ATLAS-CONF-2011-153.
106. C.T. Hill, Phys. Lett. **B266**, 419 (1991).
107. C.T. Hill, Phys. Lett. **B345**, 483 (1995).
108. T. Aaltonen (CDF Collab.), Phys. Rev. **D84**, 072004 (2011).
109. T. Aaltonen (CDF Collab.), Phys. Rev. **D84**, 072003 (2011).
110. DØ Collab., FERMILAB-PUB-05/9-E, submitted to Phys. Rev. Lett.
111. ATLAS Collab., ATLAS-CONF-2011-087.
112. ATLAS Collab., ATLAS-CONF-2011-123.
113. CMS Collab., CMS-PAS-TOP-10-007.
114. CMS Collab., CMS-PAS-EXO-11-055.
115. CMS Collab., CMS-PAS-EXO-11-0006.
116. F. Abe *et al.* (CDF Collab.), Phys. Rev. Lett. **79**, 357 (1997);
T. Affolder *et al.* (CDF Collab.), Phys. Rev. **D62**, 012004 (2000).
117. B. Abbott *et al.* (DØ Collab.), Phys. Rev. Lett. **82**, 4975 (1999);
V.M. Abazov *et al.* (DØ Collab.), Phys. Rev. Lett. **88**, 151803 (2002).
118. A. Abulencia *et al.* (CDF Collab.), Phys. Rev. Lett. **96**, 042003 (2006).
119. T. Aaltonen *et al.* (CDF Collab.), Phys. Rev. Lett. **103**, 101803 (2009).
120. V.M. Abazov *et al.* (DØ Collab.), Phys. Rev. **D80**, 071102 (2009).
121. V.M. Abazov *et al.* (DØ Collab.), Phys. Lett. **B682**, 278 (2009).
122. V.M. Abazov *et al.* (DØ Collab.), Phys. Rev. **D80**, 051107 (2009).

123. V.M. Abazov *et al.* (DØ Collab.), Phys. Rev. **D80**, 071102 (2009).
124. ATLAS Collab., ATLAS-CONF-2011-094.
125. ATLAS Collab., ATLAS-CONF-2011-138.
126. ATLAS Collab., ATLAS-CONF-2011-151.
127. ATLAS Collab., ATLAS-CONF-2011-154.
128. V.M. Abazov *et al.* (DØ Collab.), Phys. Rev. Lett. **102**, 092002 (2009).
129. V.M. Abazov *et al.* (DØ Collab.), DØ conference note 5838 (2009).
130. V.M. Abazov *et al.* (DØ Collab.), arXiv:1110.4592, submitted to Phys.Lett.B.
131. V.M. Abazov *et al.* (DØ Collab.), Phys. Lett. **B699**, 145 (2011).
132. T. Aaltonen *et al.* (CDF Collab.), Phys. Rev. Lett. **103**, 041801 (2009).
133. F. Abe *et al.* (CDF Collab.), Phys. Rev. Lett. **80**, 2525 (1998).
134. T. Aaltonen *et al.* (CDF Collab.), Phys. Rev. Lett. **101**, 192002 (2009).
135. CDF Collab., CDF conference note 9496 (2008).
136. V.M. Abazov *et al.* (DØ Collab.), Phys. Lett. **B701**, 313 (2011).
137. V.M. Abazov *et al.* (DØ Collab.), Phys. Lett. **B693**, 81 (2010).
138. A. Heister *et al.* (ALEPH Collab.), Phys. Lett. **B543**, 173 (2002); J. Abdallah *et al.* (DELPHI Collab.), Phys. Lett. **B590**, 21 (2004); P. Achard *et al.* (L3 Collab.), Phys. Lett. **B549**, 290 (2002); G. Abbiendi *et al.* (OPAL Collab.), Phys. Lett. **B521**, 181 (2001).
139. F.D. Aaron *et al.* (H1 Collab.), Phys. Lett. **B678**, 450 (2009).
140. H. Abramowics *et al.* (ZEUS Collab.), arXiv:1111.3901, submitted to Phys. Lett. B.
141. M. Beneke *et al.*, hep-ph/0003033, in *Proceedings of 1999 CERN Workshop on Standard Model Physics (and more) at the LHC*, G. Altarelli and M.L. Mangano eds.
142. V.F. Obraztsov, S.R. Slabospitsky, and O.P. Yushchenko, Phys. Lett. **B426**, 393 (1998).
143. T. Carli, D. Dannheim, and L. Bellagamba, Mod. Phys. Lett. **A19**, 1881 (2004).